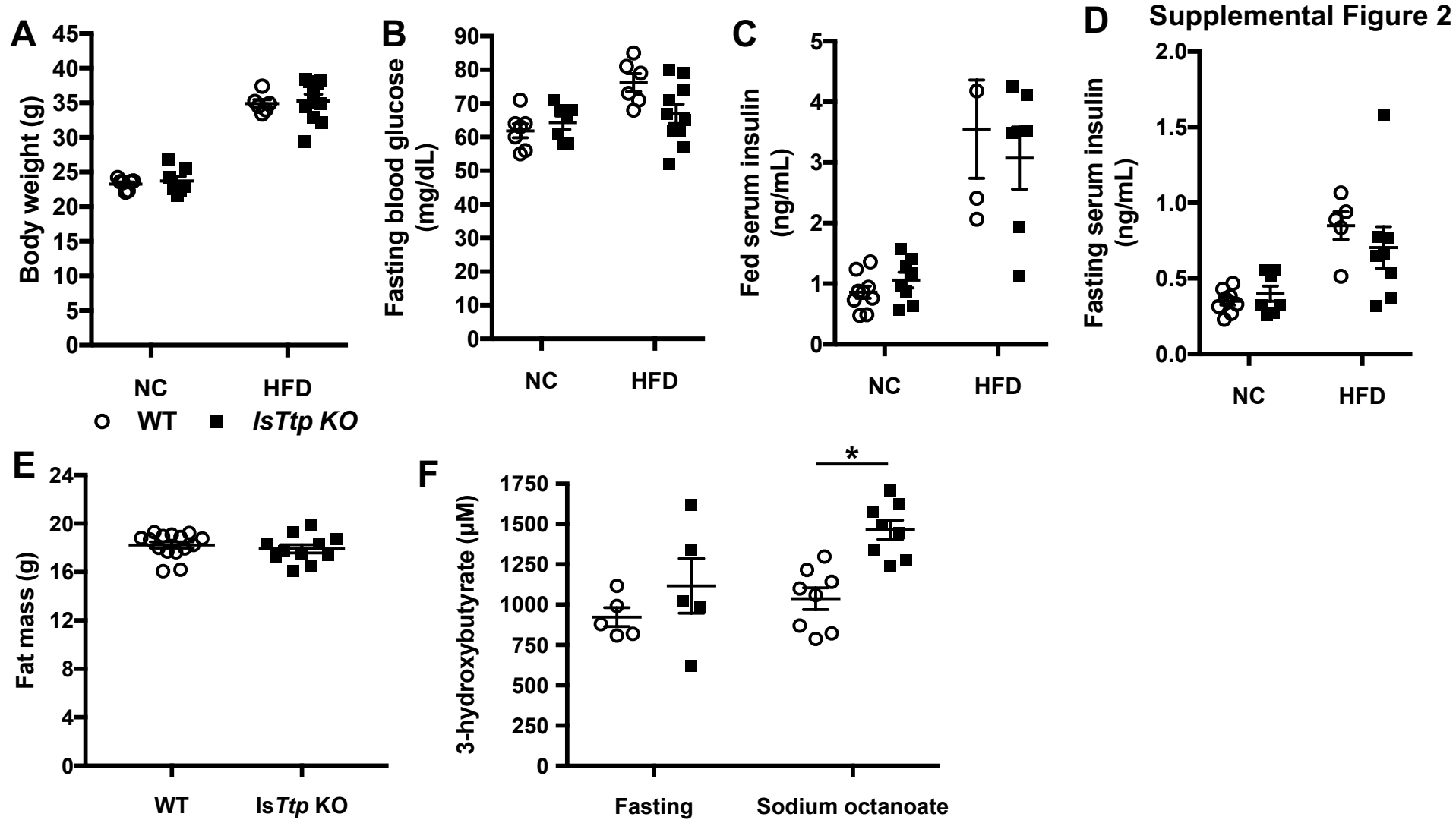


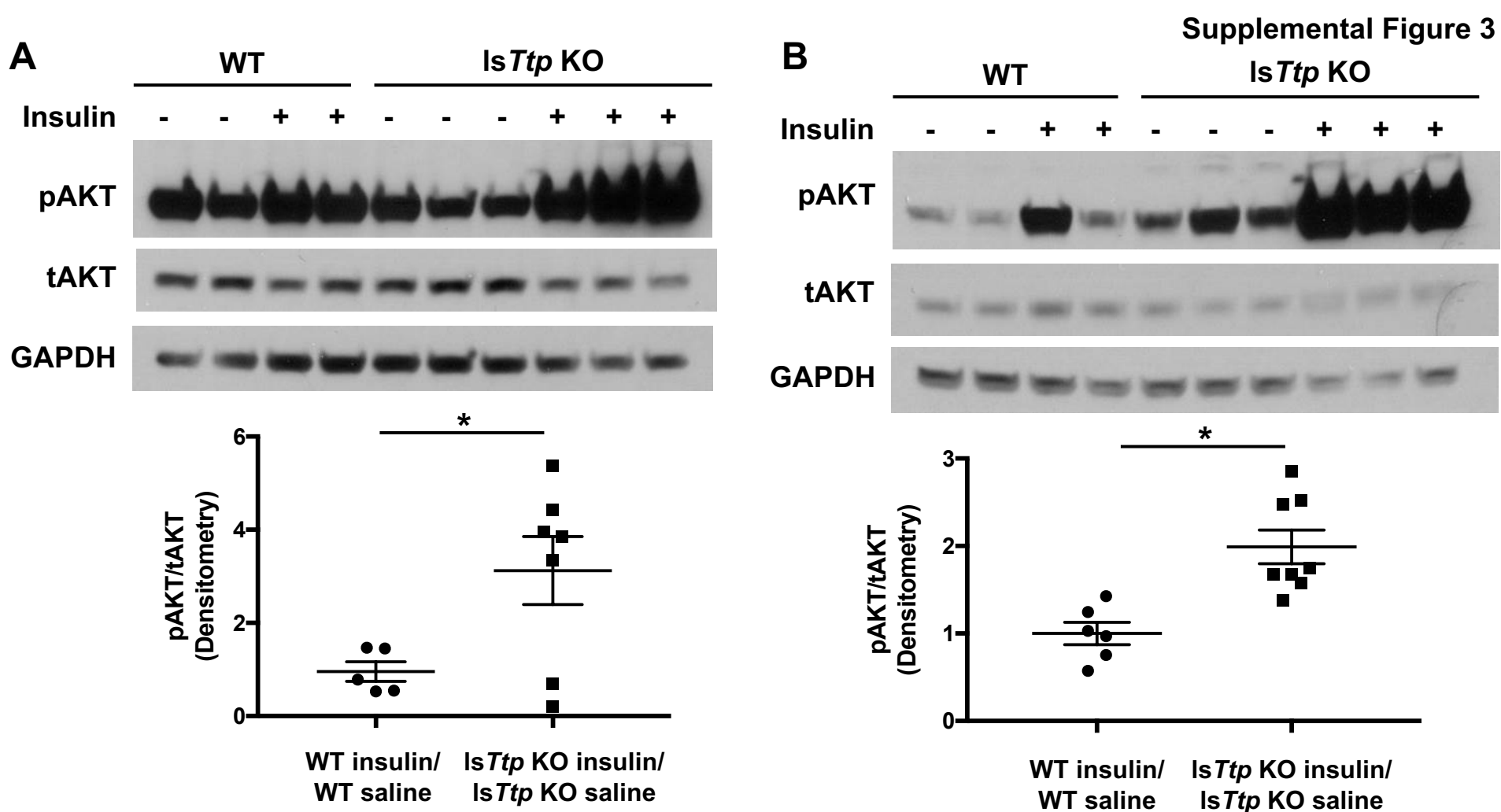
Supplemental Figure 1. Hepatic TTP is induced by insulin, and reduced in diet-induced and genetic murine models of obesity and human diabetics.

(A) *Ttp* mRNA expression is induced by 100nM insulin in a time-dependent fashion in WT primary hepatocytes (n=4). (B) *Ttp* mRNA expression is induced by insulin in a dose-dependent manner in WT primary hepatocytes (n=4). (C) TTP protein expression is induced by 100nM insulin in a time-dependent manner in WT primary hepatocytes. (D) Insulin (100nM) does not alter *Ttp* mRNA stability in WT primary hepatocytes (n=4). (E) Inhibition of protein synthesis via 2 hour pre-treatment with 0.1mM cycloheximide does not inhibit *Ttp* induction after 1 hour treatment of insulin in WT MEFs (n=4). (F) Transfection of a luciferase construct containing the proximal 137 base-pairs of the *TTP* promoter is sufficient to induce transcriptional activity compared to the full-length *TTP* promoter (n=9-10 in each group). (G) Pre-treatment of *Akt1/2* KO MEFs with a p38 MAPK inhibitor (SB 202190, 10 μ M) for one hour led to a significant reduction in *Ttp* expression after one-hour of insulin (100nM) stimulation, which was not further reduced with the addition of one-hour PKC inhibitor pre-treatment (Go 6983, 1 μ M) (n=4). Data are presented as mean \pm SEM. *p<0.05 by one-way ANOVA with *post hoc* Fisher's LSD test.

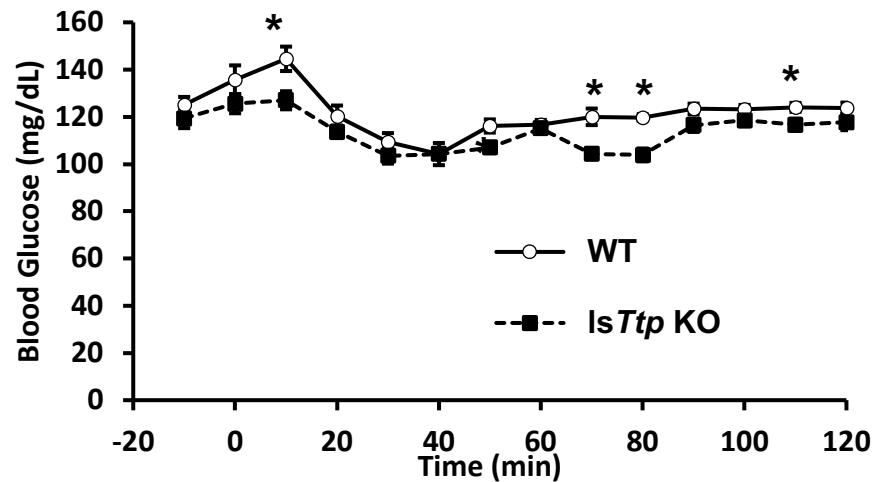
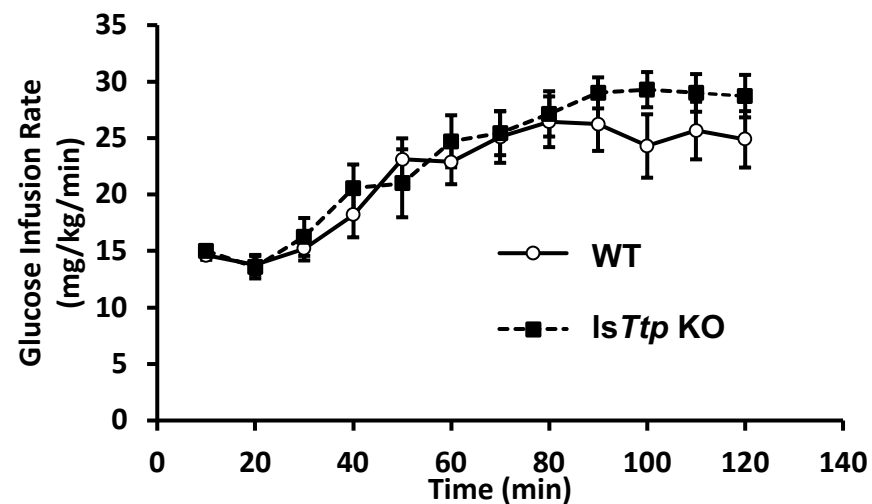
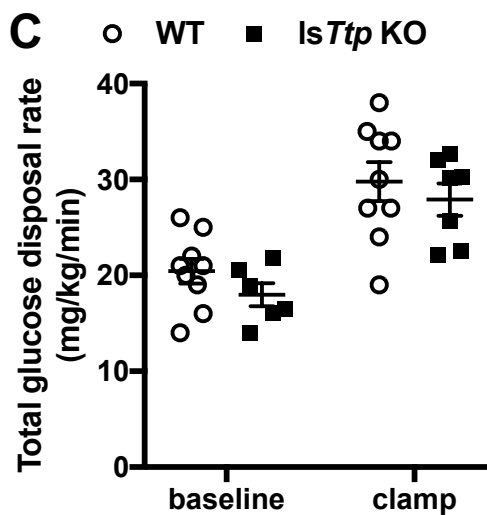
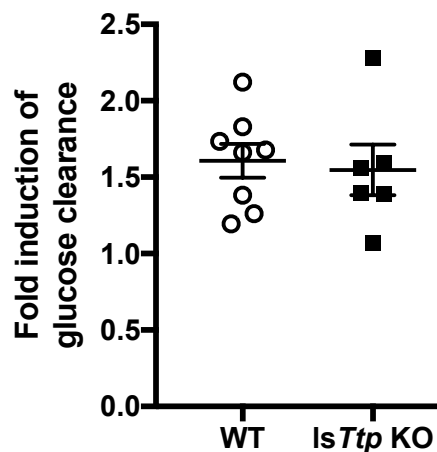
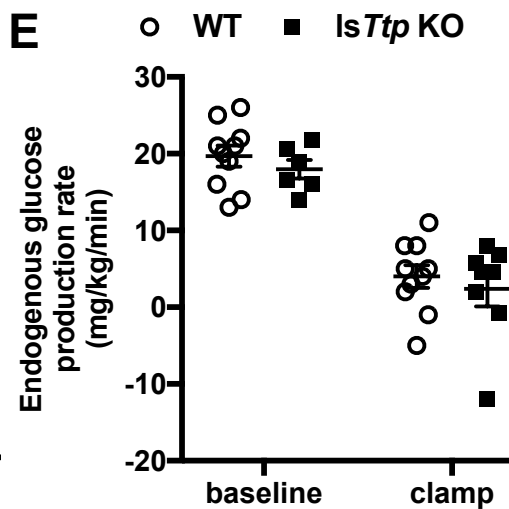
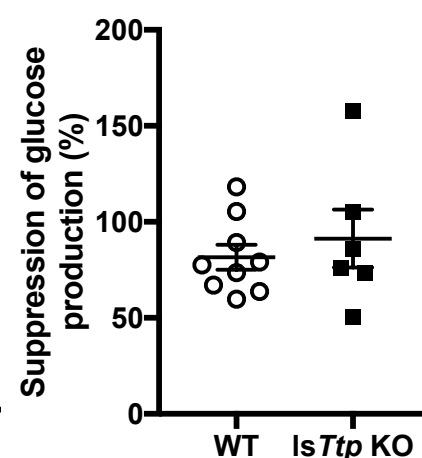


Supplemental Figure 2. Liver-specific *Ttp* KO mice have improved glucose tolerance and insulin sensitivity after high-fat diet despite normal circulating systemic lipid parameters.

(A-D) Body weight (A, n=5-10), fasting blood glucose levels (B, n=6-10), and fed (C, n=3-9) or fasting (D, n=5-9) serum insulin levels are similar between WT and *IsTtp* KO mice after 12 weeks of normal chow or high-fat diet. (E) Total fat mass in WT and *IsTtp* KO mice fed HFD (n=8-11). (F) *IsTtp* KO mice fed high-fat diet for 11 weeks have increased ketogenic potential 2 hours after injection of sodium octanoate compared to control mice (n=5-9). Data are presented as mean \pm SEM. *p<0.05 by 2-sided unpaired Student's t-test.

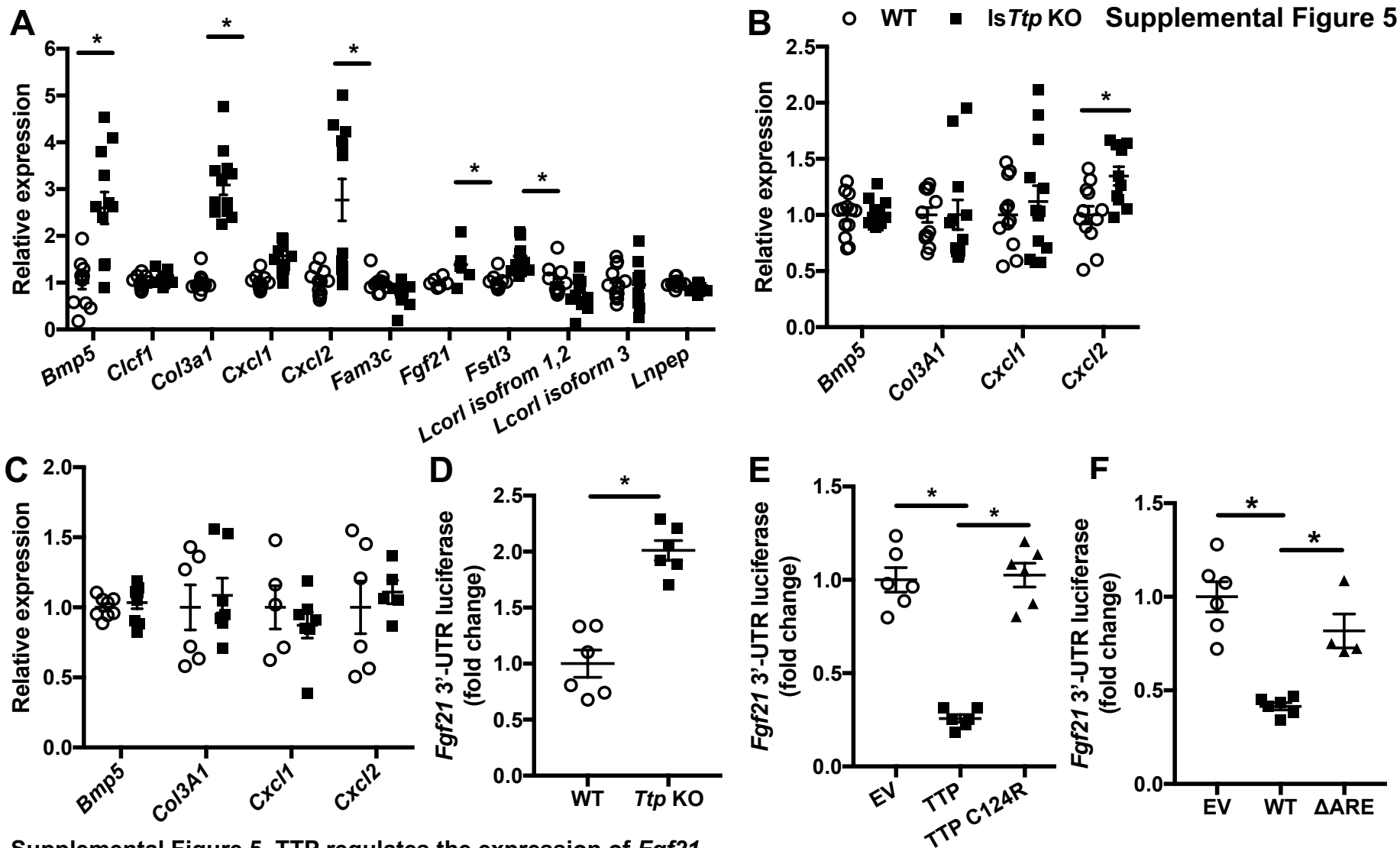


Supplemental Figure 3. Liver-specific *Ttp* KO mice have increased peripheral tissue insulin sensitivity after high-fat diet. (A-B) *IsTtp* KO mice have improved insulin sensitivity in the heart (A) and liver (B) after 12 weeks of HFD compared to WT mice, as assessed by phosphorylated AKT S473 (pAKT) to total AKT (tAKT) ratio in insulin-treated mice relative to that in saline treated-mice of the same genotype (n=6-9 in each group). Representative western blotting results are shown, and densitometry analysis is provided in the same panel. Data are presented as mean \pm SEM. * $p < 0.05$ by one-way ANOVA with *post hoc* Fisher's LSD test.

A**B****C****D****E****F**

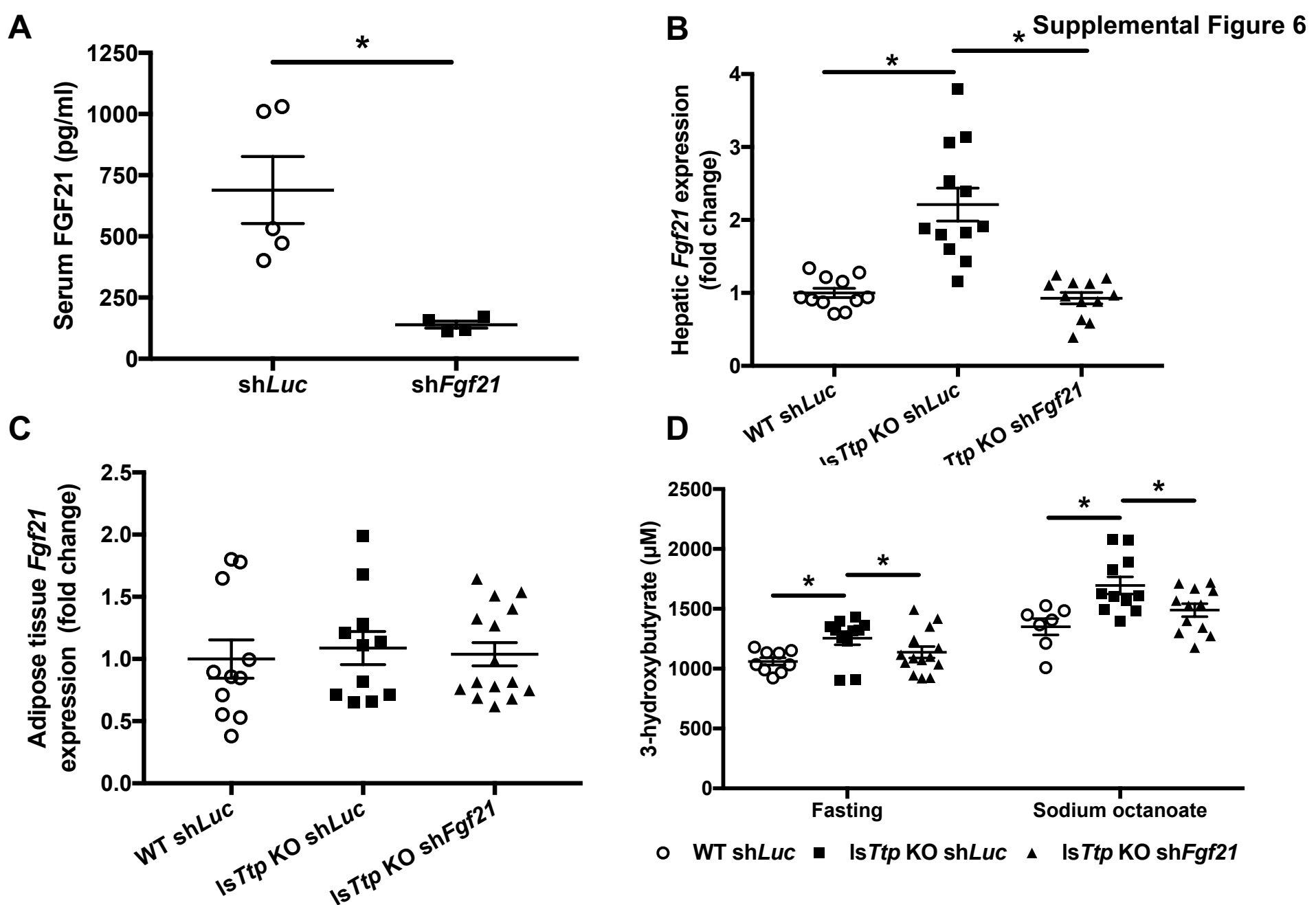
Supplemental Figure 4. Liver-specific *Ttp* KO mice have similar peripheral glucose disposal and endogenous glucose production rate after HFD compared to WT mice.

(A-B) Blood glucose (A) and glucose infusion rate (B) during hyperinsulinemic-euglycemic clamp studies. * P<0.05 by 2-tailed unpaired Student's t-test. (C) After HFD, *IsTtp* KO mice have similar total glucose disposal rate at baseline and during hyperinsulinemic-euglycemic clamp studies compared to WT mice. (D) Fold induction of glucose clearance during hyperinsulinemic-euglycemic clamp studies. (E) Endogenous glucose production at baseline and during hyperinsulinemic-euglycemic clamp studies in WT and *IsTtp* KO mice after HFD. (F) Insulin-mediated suppression of glucose production in WT and *IsTtp* KO mice during hyperinsulinemic-euglycemic clamp studies. Data are presented as mean \pm SEM. N=6-10 for each group.



Supplemental Figure 5. TTP regulates the expression of *Fgf21*.

(A) mRNA levels of predicted TTP-targeted hepatic secretory proteins in WT and *IsTtp* KO primary hepatocytes. N=6 for each group. (B) Expression of hepatic secretory proteins that are putative TTP targets in liver from WT and *IsTtp* KO mice fed regular diet. N=10-12 for each group. (C) Expression of putative TTP-targeted hepatic secretory proteins in WT and *IsTtp* KO mice after 15 weeks of HFD. (D) Transfection of a mouse *Fgf21* 3'-UTR-luciferase construct into *Ttp* KO MEFs increases luminescence signal compared to WT MEFs (n=6). (E) Overexpression of WT TTP but not C124R mutant TTP reduces luciferase activity in HEK293 cells transfected with mouse *Fgf21* 3'-UTR-luciferase construct (n=6). (F) TTP overexpression in *Ttp* KO MEFs reduces the activity of mouse *Fgf21* 3'-UTR-luciferase construct (WT) but not mouse *Fgf21* 3'-UTR-luciferase construct with deletions of the ARE sites (Δ ARE). n=5-6. Data presented as the relative luciferase activity in the presence of TTP overexpression for each construct. EV= empty pMIR-Report vector. Data are presented as mean \pm SEM. * $p < 0.05$ by one-way ANOVA with *post hoc* Fisher's LSD test.



Supplemental Figure 6. Increased liver-derived circulating Fgf21 is responsible for improved systemic diabetic parameters after high fat diet in the setting of hepatic *Ttp* deletion.

(A) Circulating fasting levels of FGF21 are effectively reduced using AAV8 sh*Fgf21* in WT mice on normal chow (n=4-5). (B-C) AAV8 sh*Fgf21* specifically reduces hepatic (B), but not adipose tissue (C), *Fgf21* mRNA expression in *IsTtp* KO mice (n=11-14). (D) *IsTtp* KO mice injected with AAV8 sh*Fgf21* virus have reversal of ketogenic potential after HFD compared to WT mice (n=7-12). Data are presented as mean \pm SEM. * $p < 0.05$ by one-way ANOVA with *post hoc* Fisher's LSD test.